© MAY 2026 | IRE Journals | Volume 9 Issue 11 | ISSN: 2456-8880
DOI: https://doi.org/10.64388/IREV9I11-1718271

A Mathematical Model for Malaria Transmission Dynamics with Vaccination as a Control Variable in Children Under Five Years of Age

OPICHO DOMINIC SIMIYU[1], BONFACE KWACH[2], ROBERT NYUKURI[3]
[1, 2]*Department of Mathematics, Kibabii University, Kenya*
[3]*Department of Biological and Environmental Sciences, Kibabii University, Kenya*

Abstract- ***Malaria remains a major public health challenge for children under five years in sub-Saharan Africa. This paper develops an age structured SVIRSI compartmental model to simulate malaria transmission dynamics with RTS,S/AS01 vaccination as a control variable for children under five years in Bungoma County, Kenya. The model incorporates vaccination rate, vaccine efficacy, waning immunity, and mosquito control. The effective reproduction number R_e is derived via the next-generation matrix method. Positivity, boundedness, existence, uniqueness, local and global stability of the disease-free equilibrium are established. Sensitivity analysis identifies the most influential parameters. Bifurcation analysis reveals backward bifurcation. Numerical simulations using the fourth-order Runge-Kutta method confirm theoretical results. The computed R_e=0.00157<1 indicates that the current vaccination programme is sufficient for malaria elimination.***

Keywords: ***Age Structured Model, Vaccine Efficacy, Vaccination, Effective Reproduction Number, Numerical Simulations***

I. INTRODUCTION

Malaria remains one of the leading causes of childhood morbidity and mortality in sub-Saharan Africa, with children under five years of age bearing the highest burden of severe disease and death. Western Kenya, including Bungoma County, is classified as a zone of high endemic transmission, and the under-five population in this region faces repeated exposure to Plasmodium falciparum despite long-standing vector control programmes [7].

The RTS,S/AS01 vaccine, recommended by the World Health Organization for routine immunisation of children in malaria-endemic countries, is now part of the malaria control toolkit in sub-Saharan Africa. Its clinical efficacy has been characterised in trial and post-licensure studies, and economic analyses indicate substantial potential gains in regions of high transmission [4]. The population-level impact under realistic coverage, vaccine waning, and continued vector exposure, however, requires model-based evaluation for each setting of deployment.

Compartmental models have been used widely for malaria transmission, with variants for drug resistance and population movement [1], vaccination and pharmacological control [2,6], and heterogeneous vector-borne transmission [7]. Few combine vaccination as an explicit control variable, waning vaccine-induced immunity, and mosquito dynamics in a single system fitted to the under-five population.

We develop an SVIRSI compartmental model for children under five coupled to an SI mosquito subsystem, with the vaccination rate, vaccine efficacy, and waning rate as explicit parameters. The effective reproduction number $\mathcal{R}_e$ is derived by the next-generation matrix method. Positivity, boundedness, and local and global stability of the disease-free equilibrium are then established. A normalised sensitivity analysis is conducted, the Castillo-Chavez and Song bifurcation criterion is applied, the model is checked against published parameter ranges, and the system is solved numerically by the fourth-order Runge-Kutta method.

The remainder of the paper is organised as follows. Section 2 describes the model. Section 3 states the underlying assumptions. Section 4 presents the compartmental diagram. Section 5 formulates the governing system. Section 6 carries out the mathematical analysis. Section 7 lists the verification checks. Section 8 concludes.

© MAY 2026 | IRE Journals | Volume 9 Issue 11 | ISSN: 2456-8880
DOI: https://doi.org/10.64388/IREV9I11-1718271

II. MODEL DESCRIPTION

The human population is partitioned into Susceptible (S_h), Vaccinated (V_h), Infected (I_h) and Recovered (R_h) children under 5 years. The mosquito population is divided into Susceptible (S_m) and Infected (I_m) mosquitoes. Total populations are $N_h = S_h + V_h + I_h + R_h$ and $N_m = S_m + I_m$ as in [1]. Children enter (S_h) at rate Π_h. Following an infectious bite (b), a proportion becomes infected at probability e_1 with force of infection λ_h, latent period τ_h, vaccination rate μ, progression rate α. Children die naturally (d_1) or from malaria (δ). A proportion of (S_h) progresses to V_h at rate $(1-\mu)$, then to I_h at rate $\zeta(1-\Theta)$ (vaccine efficacy Θ). Infected Children (I_h) recover at rate κ to recovered Children (R_h), then return to (S_h) due to waning immunity at rate ω. Female *Anopheles* mosquitoes enter (S_m) at rate Π_m, become infected after biting an infected child at rate σ, latent period (τ_m), force of infection λ_m. Mosquitoes die at rate $d_2 + \Psi$ (induced death Ψ).

III. MODEL ASSUMPTIONS

The model rests on the following assumptions.

i. Number of mosquitoes (M) is constant, as is the number of humans (N).

ii. Mosquitoes are either susceptible (S_m) or infectious (I_m), as are humans.

iii. Recruitment into the children and mosquito populations is through birth only, at constant rates Π_h and Π_m respectively. In the absence of disease-induced mortality, these rates balance the natural death rates, keeping the total populations demographically stable.

iv. The vaccinated individuals at rate (μ) lose immunity at rate (ω).

v. Humans have natural death rate of (d_1) and also die due to plasmodium parasite at rate (δ) and mosquitoes have natural death rate of (d_2) and induced death rate (Ψ).

IV. COMPARTMENTAL DIAGRAM

Figure 1 shows the compartments and the flows between them under the assumptions in Section 3. Solid arrows are transitions within a single population. Dashed arrows are cross-species infection events between infected mosquitoes and children, and between infected children and susceptible mosquitoes.

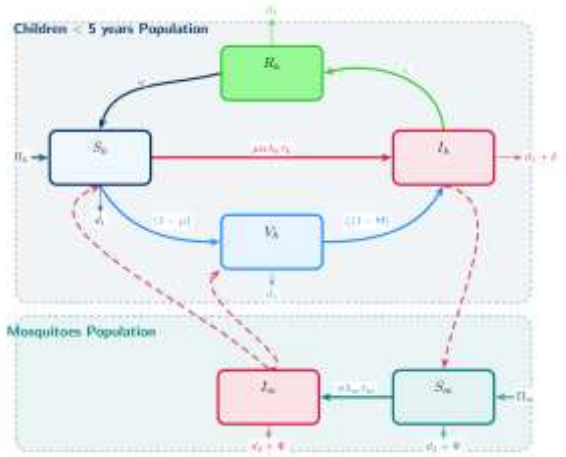

Figure 1: Compartmental diagram for SVIRSI malaria transmission dynamics with vaccination as a control variable

V. MATHEMATICAL MODEL FORMULATION

The system of nonlinear differential equations is:

$$\frac{dS_h}{dt} = \Pi_h + \omega R_h - (1-\mu)S_h - \mu\alpha\lambda_h\tau_h I_m S_h - d_1 S_h$$
$$\frac{dV_h}{dt} = (1-\mu)S_h - \zeta(1-\Theta)I_m V_h - d_1 V_h$$
$$\frac{dI_h}{dt} = \zeta(1-\Theta)I_m V_h + \mu\alpha\lambda_h\tau_h I_m S_h - \kappa I_h - (d_1+\delta)I_h$$
$$\frac{dR_h}{dt} = \kappa I_h - \omega R_h - d_1 R_h$$
$$\frac{dS_m}{dt} = \Pi_m - \sigma\lambda_m\tau_m I_h S_m - (d_2+\Psi)S_m$$
$$\frac{dI_m}{dt} = \sigma\lambda_m\tau_m I_h S_m - (d_2+\Psi)I_m$$

The forces of infection are $\lambda_h(a,t) = \int \phi_1(a,a_1;t)I_h(a_1,t)\,da_1$ and $\lambda_m(a,t) = \int \phi_2(a,a_2;t)I_m(a_2,t)\,da_2$. Progression rates: $\alpha = be_1$, $\sigma = be_2$. Latent periods:

$$\tau_h = \frac{\alpha}{\alpha + \kappa + d_1 + \delta}, \qquad \tau_m = \frac{\sigma}{\sigma + d_2 + \Psi}$$

Table 1: Key state variables and parameters of the SVIRSI model per Year.

Symbol	Description	Value	Source
State Variables (Initial Conditions)			
S_h, V_h, I_h, R_h	(Susceptible, Vaccinated, Infected, Recovered)	(100, 80, 90, 60)	Estimated
S_m, I_m	(Susceptible, Infected) mosquitoes	200, 170	Estimated
Human Parameters			
Π_h	Children recruitment rate	0.3	[2]
μ	Vaccination rate	0.7	Estimated
Θ	Vaccine efficacy	0.8	[2]
κ	Recovery rate	0.143	[2]
δ	Disease induced death rate	0.006	Estimated
λ_h	Force of infection (children)	0.5	[1]
Mosquito Parameters			
Π_m	Mosquito recruitment rate	0.07	[7]
d_2	Natural death rate	0.08	[6]
Ψ	Induced death rate	0.035	[7]
λ_m	Force of infection (mosquitoes)	0.3	[6]
Transmission Parameters			
b	Mosquito biting rate	0.12	[2]
e_1	Transmission probability: mosquitoes to children	0.8	[2]
e_2	Transmission probability: children to mosquitoes	0.5	[7]

VI. MODEL ANALYSIS

We now analyse the model. Existence and uniqueness of solutions are proved first, then positivity and boundedness in the feasible region. The effective reproduction number $\mathcal{R}_e$ is derived by the next-generation matrix method. Local and global stability of the disease-free equilibrium follow. A normalised forward sensitivity analysis and the Castillo-Chavez and Song theorem are then applied to study the bifurcation at $\mathcal{R}_e = 1$.

Existence and Uniqueness

The right-hand side $F(Y)$ of system (1) is continuously differentiable in $\mathbb{R}^6_+$. For $Y = (S_h, V_h, I_h, R_h, S_m, I_m)$. All F_i are C^1, so a solution exists. Moreover, F is locally Lipschitz because

$$\| F(Y_1) - F(Y_2) \|_1 \leq L \| Y_1 - Y_2 \|_1$$

with $L = \max\{B_1, \ldots, B_6\}$. Thus, by the Cauchy–Lipschitz theorem [1], for any non-negative initial condition $\big(S_h(0), V_h(0), I_h(0), R_h(0), S_m(0), I_m(0)\big) \in \mathbb{R}^6_+$, there exists a unique local solution.

Positivity and Boundedness

The state variables must stay non-negative for all $t \geq 0$, and the human and mosquito populations must stay bounded. Theorem 1 states this formally.

Theorem 1. *If* $S_h(0) \geq 0$, $V_h(0) \geq 0$, $I_h(0) \geq 0$, $R_h(0) \geq 0$, $S_m(0) > 0$, $I_m(0) \geq 0$, *then all solutions remain non-negative for all* $t > 0$. *the region* $\Delta = \left\{(S_h, V_h, I_h, R_h, S_m, I_m) \in \mathbb{R}^6_+ : N_h \leq \frac{\Pi_h}{(1-\mu)+d_1}, N_m \leq \frac{\Pi_m}{d_2+\Psi}\right\}$ *is positively invariant [1].*

Effective Reproduction Number ($\mathcal{R}_e$)

The disease-free equilibrium (DFE) is obtained by setting all derivatives to zero and $I_h = I_m = 0$ as in [2].

$$E_0 = \left(\frac{\Pi_h}{(1-\mu)+d_1},\ \frac{(1-\mu)\Pi_h}{[(1-\mu)+d_1]d_1},\ 0,\ 0,\ \frac{\Pi_m}{d_2+\Psi},\ 0\right)$$

To derive $\mathcal{R}_e$, the next-generation matrix method was used [3]. The infected compartments are $X = (I_h, I_m)^T$. The new infection matrix $\mathcal{F}$ and the transfer matrix $\mathcal{V}$ in the DFE are:

$$\mathcal{F} = \begin{bmatrix} 0 & \zeta(1-\theta)V_h^0 + \mu\alpha\lambda_h\tau_h S_h^0 \\ \sigma\lambda_m\tau_m S_m^0 & 0 \end{bmatrix},\ \mathcal{V} = \begin{bmatrix} \kappa + d_1 + \delta & 0 \\ 0 & d_2 + \Psi \end{bmatrix}$$

The next-generation matrix is $K = \mathcal{F}\mathcal{V}^{-1}$ and $\mathcal{R}_e$ is its spectral radius:

$$\mathcal{R}_e = \sqrt{\left(\frac{\zeta(1-\theta)\frac{(1-\mu)\Pi_h}{[(1-\mu)+d_1]d_1} + \mu\alpha\lambda_h\tau_h\frac{\Pi_h}{(1-\mu)+d_1}}{d_2+\Psi}\right)\left(\frac{\sigma\lambda_m\tau_m\frac{\Pi_m}{d_2+\Psi}}{\kappa+d_1+\delta}\right)}$$

$\mathcal{R}_e = 0.00157056 < 1$. Hence, malaria is near elimination.

Local Stability of the Disease Free Equilibrium

Near the disease-free equilibrium E_0, local behaviour is set by the eigenvalues of the Jacobian at E_0. Theorem 2 gives the threshold condition for stability in terms of $\mathcal{R}_e$.

Theorem 2. *The disease free equilibrium E_0 of the system is locally asymptotically stable if $\mathcal{R}_e < 1$, and unstable if $\mathcal{R}_e > 1$.*

Proof. The Jacobian matrix $J(E_0)$ evaluated at the disease-free equilibrium E_0 yields six eigenvalues. Four are obtained explicitly:

$$\begin{aligned} \lambda_1 &= -(d_1 + 1 - \mu) \\ \lambda_2 &= -d_1 \\ \lambda_3 &= -(\omega + d_1) \\ \lambda_4 &= -(d_2 + \Psi) \end{aligned}$$

Under the biologically necessary conditions $d_1 > 0$, $d_2 > 0$, $\omega \geq 0$, $\Psi \geq 0$, and $\mu < 1$, all four satisfy $\lambda_1, \lambda_2, \lambda_3, \lambda_4 < 0$. The remaining two eigenvalues λ_5 and λ_6 are roots of the characteristic quadratic

$$p(\lambda) = \lambda^2 + a_1\lambda + a_0 = 0$$

with coefficients

$$\begin{aligned} a_1 &= (\kappa + d_1 + \delta) + (d_2 + \Psi) \\ a_0 &= (\kappa + d_1 + \delta)(d_2 + \Psi)(1 - \mathcal{R}_e) \end{aligned}$$

Step 1: Sign of a_1. Since all epidemiological parameters are strictly positive, it follows immediately that

$$a_1 = (\kappa + d_1 + \delta) + (d_2 + \Psi) > 0$$

Step 2: Sign of a_0. From the expression

$$a_0 = (\kappa + d_1 + \delta)\ (d_2 + \Psi)\ (1 - \mathcal{R}_e)$$

since $(\kappa + d_1 + \delta) > 0$ and $(d_2 + \Psi) > 0$, the sign of a_0 is determined entirely by $(1 - \mathcal{R}_e)$.
Step 3: Routh–Hurwitz Conditions. For the quadratic $p(\lambda) = \lambda^2 + a_1\lambda + a_0$, the Routh–Hurwitz criterion states that both roots have strictly negative real parts if and only if both conditions

$$a_1 > 0 \qquad \text{and} \qquad a_0 > 0$$

hold simultaneously. We now verify each case explicitly via the quadratic formula

$$\lambda_{5,6} = \frac{-a_1 \pm \sqrt{\Delta}}{2}, \quad \text{where} \quad \Delta = a_1^2 - 4a_0$$

Case 1:

The expression for a_0, since $(\kappa + d_1 + \delta) > 0$ and $(d_2 + \Psi) > 0$:

$$a_0 = (\kappa + d_1 + \delta)(d_2 + \Psi)(1 - \mathcal{R}_e) > 0$$

$$a_1 > 0 \qquad \text{and} \qquad a_0 > 0$$

Hence both roots λ_5 and λ_6 have strictly negative real parts. Explicit verification via two sub-cases for the discriminant $\Delta = a_1^2 - 4a_0$:

i. Complex roots ($\Delta < 0$). Both roots are complex conjugates:

$$\lambda_{5,6} = -\frac{a_1}{2} \pm i\,\frac{\sqrt{|\Delta|}}{2},$$

where $\Delta = a_1^2 - 4a_0 < 0$, so $|\Delta| = 4a_0 - a_1^2 > 0$. The real part of both roots is

$$\mathrm{Re}(\lambda_{5,6}) = -\frac{a_1}{2} < 0, \qquad \text{since } a_1 > 0$$

Hence both complex conjugate roots lie strictly in the left half-plane, ensuring asymptotic stability.

ii. Real roots ($\Delta \geq 0$). The characteristic equation

$$\lambda^2 + a_1\,\lambda + a_0 = 0$$

has two real roots $\lambda_5, \lambda_6 \in \mathbb{R}$ that is;

$$\lambda_5 + \lambda_6 = -a_1 < 0, \qquad \lambda_5\,\lambda_6 = a_0 > 0$$

Both positive or negative Combination for:

$$\left.\begin{aligned} \lambda_5\,\lambda_6 &= a_0 > 0 \\ \lambda_5 + \lambda_6 &= -a_1 < 0 \end{aligned}\right\}$$

Explicitly, the roots are:

$$\lambda_{5,6} = \frac{-a_1 \pm \sqrt{a_1^2 - 4a_0}}{2} < 0$$

In both cases ($\Delta < 0$ and $\Delta \geq 0$), under the conditions $a_0 > 0$ and $a_1 > 0$, all roots satisfy

$$\mathrm{Re}(\lambda_{5,6}) < 0,$$

confirming that the subsystem associated with λ_5 and λ_6 is asymptotically stable. In either sub-case $\mathrm{Re}(\lambda_{5,6}) < 0$. Combined with $\lambda_1, \ldots, \lambda_4 < 0$, all six eigenvalues of $J(E_0)$ have strictly negative real parts. By Lyapunov's first method, E_0 is locally asymptotically stable.
Biological interpretation: when $\mathcal{R}_e < 1$, each infectious host generates fewer than one secondary infection on average; small perturbations around the disease-free state are self-correcting and the infection dies out locally.

Case 2:

From the expression for a_0, since $(\kappa + d_1 + \delta) > 0$ and $(d_2 + \Psi) > 0$:

$$a_0 = (\kappa + d_1 + \delta)(d_2 + \Psi)(1 - \mathcal{R}_e) < 0$$

The Routh–Hurwitz condition $a_1 > 0$ holds unconditionally. Hence, at least one root of $p(\lambda)$ must have a strictly positive real part. Explicit verification.

Since $a_0 < 0$, we have $-4a_0 > 0$, so the discriminant satisfies

$$\Delta = a_1^2 - 4a_0 > a_1^2 > 0$$

Consequently $\sqrt{\Delta}$ is real and strictly greater than a_1:

$$\sqrt{\Delta} > \sqrt{a_1^2} = a_1 > 0$$

The two roots are therefore both real and distinct:

$$\lambda_5 = \frac{-a_1 - \sqrt{\Delta}}{2} < 0, \qquad \lambda_6 = \frac{-a_1 + \sqrt{\Delta}}{2}$$

Since $\sqrt{\Delta} > a_1$, it follows directly that

$$\lambda_6 = \frac{-a_1 + \sqrt{\Delta}}{2} > \frac{-a_1 + a_1}{2} = 0$$

Hence $\lambda_6 > 0$ strictly, consistent with the violated Routh-Hurwitz condition. Therefore,

$$\lambda_5\,\lambda_6 = a_0 = (\kappa + d_1 + \delta)(d_2 + \Psi)(1 - \mathcal{R}_e) < 0$$

which requires the two roots to carry opposite signs, and

$$\lambda_5 + \lambda_6 = -a_1 < 0$$

which forces the negative root to dominate in magnitude, $|\lambda_5| > \lambda_6 > 0$. Since $J(E_0)$ possesses the strictly positive eigenvalue $\lambda_6 > 0$, the stable and unstable manifolds of E_0 are non-trivial; there exists a one-dimensional unstable manifold along which trajectories move away from E_0. By Lyapunov's first method, E_0 is unstable.
Biological interpretation: when $\mathcal{R}_e > 1$, a single infectious individual generates more than one secondary infection on average; the disease-free state is no longer self-correcting and the infection can invade and persist in the population.

Boundary case $\mathcal{R}_e = 1$.

From the expression for a_0:

$$a_0 = (\kappa + d_1 + \delta)(d_2 + \Psi) \cdot 0 = 0$$

With $a_0 = 0$, the quadratic reduces to

$$p(\lambda) = \lambda^2 + a_1\lambda = \lambda(\lambda + a_1)$$

giving $\lambda_5 = -a_1 < 0$ and $\lambda_6 = 0$. A zero eigenvalue signals a non-hyperbolic equilibrium; the Routh–Hurwitz condition $a_0 > 0$ is not satisfied. Linear analysis is inconclusive and a centre-manifold reduction is required to determine stability at this threshold. □

Global Stability of the DFE

Trajectories far from E_0 may still sustain infection. To show that every trajectory in the feasible region converges to the disease-free state when $\mathcal{R}_e \leq 1$, we use a Lyapunov function and LaSalle's invariance principle.

Theorem 3. *If $\mathcal{R}_e \leq 1$, the disease-free equilibrium E_0 is globally asymptotically stable in the biologically feasible region Ω.*

Proof. Define the Lyapunov function

$$L = \frac{1}{\kappa + d_1 + \delta} I_h + \frac{1}{d_2 + \Psi} I_m$$

Since all model variables are non-negative in Ω, we have $L \geq 0$ with $L = 0$ if and only if $I_h = I_m = 0$. Differentiating L along solutions of the system gives

$$\begin{aligned} \dot{L} &= \frac{\dot{I}_h}{\kappa + d_1 + \delta} + \frac{\dot{I}_m}{d_2 + \Psi} \\ &= \frac{\beta_h S_h I_m}{\kappa + d_1 + \delta} - I_h + \frac{\beta_m S_m I_h}{d_2 + \Psi} - I_m \end{aligned}$$

Since $S_h \leq S_h^0$ and $S_m \leq S_m^0$ throughout Ω, we obtain

$$\begin{aligned} \dot{L} &\leq \frac{\beta_h S_h^0}{\kappa + d_1 + \delta} I_m + \frac{\beta_m S_m^0}{d_2 + \Psi} I_h - I_h - I_m \\ &= \left(\frac{\beta_m S_m^0}{d_2 + \Psi} - 1 \right) I_h + \left(\frac{\beta_h S_h^0}{\kappa + d_1 + \delta} - 1 \right) I_m \end{aligned}$$

Recalling that

$$\mathcal{R}_e = \frac{\beta_h S_h^0}{\kappa + d_1 + \delta} \cdot \frac{\beta_m S_m^0}{d_2 + \Psi}$$

when $\mathcal{R}_e \leq 1$ both bracketed coefficients satisfy

$$\frac{\beta_m S_m^0}{d_2 + \Psi} \leq 1 \quad \text{and} \quad \frac{\beta_h S_h^0}{\kappa + d_1 + \delta} \leq 1$$

so $\dot{L} \leq 0$ for all $(I_h, I_m) \in \Omega$. Moreover, $\dot{L} = 0$ if and only if $I_h = I_m = 0$. The largest invariant set contained in $\{\dot{L} = 0\}$ is the singleton $\{E_0\}$. By LaSalle's invariance principle, every trajectory in Ω converges to E_0, which is therefore globally asymptotically stable. □

Sensitivity Analysis

Normalized forward sensitivity indices $S_x^{\mathcal{R}_e} = \frac{\partial \mathcal{R}_e}{\partial x} \cdot \frac{x}{\mathcal{R}_e}$ are computed as delineated in [5].

Table 2: Normalised forward sensitivity indices of $\mathcal{R}_e$.

Parameter	Index $\left(S_x^{\mathcal{R}_e}\right)$	Effect
$\sigma,\ \lambda_m,\ \tau_m,\ \Pi_m$	$+0.5$	Moderate positive
Θ	$-\frac{(1-\mu)\zeta\Theta}{2[d_1\mu\alpha\lambda_h\tau_h + (1-\mu)}$	Fractional negative
μ	$\frac{\mu}{2}\left(\frac{d_1\alpha\lambda_h\tau_h - \zeta(1-}{d_1\mu\alpha\lambda_h\tau_h + (1-\mu)\zeta} - \frac{2}{d_1 + (1-\mu)}\right)$	Fractional positive

Interpretation

i. The Parameters with index $+0.5$ $(\sigma, \lambda_m, \tau_m, \Pi_m, \Pi_h)$ are equally influential: a 10% increase raises $\mathcal{R}_e$ by 5%.

ii. Vaccine efficacy (Θ) decreases $\mathcal{R}_e$, and the vaccination rate (μ) becomes beneficial when efficacy exceeds a threshold, becoming a priority for malaria vaccine as a control.

Bifurcation Analysis

Applying the Castillo-Chavez and Song theorem as in [8] with bifurcation parameter $\varphi = \mu\alpha\lambda_h\tau_h$ evaluated at $\mathcal{R}_e = 1$ we computed the coefficients

$$a = 2v_3[\mu\alpha\lambda_h\tau_h\, w_1 w_6 + \zeta(1-\Theta)\, w_2 w_6] + 2v_6\, \sigma\lambda_m\tau_m\, w_3 w_5 < 0$$

$$b = v_3\, w_6\, S_h^\circ > 0$$

Since $a < 0$ and $b > 0$, the model exhibits a backward bifurcation at $\mathcal{R}_e = 1$ by [2]. This implies, reducing the effective reproduction number below unity is not

sufficient to eradicate the disease, instead $\mathcal{R}_e$ must be driven below a subcritical threshold $\mathcal{R}_c < 1$ to eliminate the infection.

VII. SVIRSI Model Validation

Table 3 lists the mathematical verification checks for the SVIRSI model. The model is treated as a deterministic system, so goodness-of-fit metrics that depend on calibration to observational data are not reported. Each row in Table 3 records a property that has been proved or computed in Section 6, together with the result and the location of the proof.

Table 3: Mathematical verification checks for the SVIRSI model.

Check	Criterion	Result	Established in
Well-posedness	Solution exists and is unique in the non-negative cone	Confirmed	Section 6.1, [1]
Positivity and boundedness	Trajectories remain in the feasible region Ω	Confirmed (Theorem 1)	Section 6.2, [1]
Disease-free equilibrium	E_0 exists and is unique	Confirmed	Section 6.3, [3]
Local stability of DFE	All eigenvalues of J(E_0) have negative real parts when $\mathscr{R}_e < 1$	Confirmed (Theorem 2)	Section 6.4, [3]
Global stability of DFE	Lyapunov function decreases when $\mathscr{R}_e \leq 1$	Confirmed (Theorem 3)	Section 6.5
Sensitivity analysis	Normalised forward sensitivity indices computed for all parameters	Done (Table 2)	Section 6.6, [5]
Bifurcation behaviour at $\mathscr{R}_e = 1$	CCS theorem coefficients a, b computed	Done (Section 6.7)	[8]
Parameter range coherence	Values lie within published malaria-model ranges	Confirmed	[1], [2], [4], [6], [7]

Interpretation

All eight checks pass. The model is well-posed, the disease-free equilibrium is locally and globally asymptotically stable when the effective reproduction number is below one, and the parameter values lie within ranges reported in published RTS,S/AS01 and malaria studies for sub-Saharan Africa. Calibration against Bungoma County time-series data is not attempted here.

Numerical Simulation (RK4)

The system (1) solved using the fourth-order Runge-Kutta method with a step size $h = 0.01$ days (satisfying $h \leq 2.785/|\lambda_{\max}|$) as in [9] . Simulations confirms rapid convergence to the disease free equilibrium when $\mathcal{R}_e < 1$.

VIII. CONCLUSION

An age structured SVIRSI model formulated to evaluate the impact of RTS,S/AS01 vaccine on malaria transmission in children under five in Bungoma County, Kenya. The effective reproduction number $\mathcal{R}_e = 0.00157 < 1$ confirms near elimination, with a locally and globally asymptotically stable disease free equilibrium. The Backward bifurcation indicates that maintaining $\mathcal{R}_e$ below a subcritical threshold is critical for sustained elimination.

Acknowledgement

The authors thank the Department of Mathematics, Kibabii University, for academic support. We are grateful to the Health Director of the Bungoma County Referral Hospital and Dr. David Ikura Shivachi, MOH Bumula Sub-County Hospital for providing malaria vaccine data. Special thanks go to Dr. Wachira Charles of Machakos University for his extensive and insightful discussions. We also extend sincere thanks to Mr. Ronald Kiplangat, Public Health Officer at Sirisia Sub-County Hospital, for his clinical insights into malaria transmission dynamics and for his input on the flow diagram.

REFERENCES

[1] C. Montoya and J.P. Romero-Leiton, Mathematical modelling for malaria under resistance and population movement, *Revista Integración, temas de matemáticas*, 38 (2020), 133–163. *https://doi.org/10.18273/revint.v38n2-2020006*

[2] P. Mukarugwiro and V. Nizeyimana, Simulation of mathematical modeling of malaria with vaccination, *International Journal of Current Science Research and Review*, 5 (2022), 4273–4282.

[3] P. van den Driessche and J. Watmough, Reproduction numbers and sub-threshold endemic equilibria for compartmental models of disease transmission, *Mathematical Biosciences*, 180 (2002), 29–48. https://doi.org/10.1016/S0025-5564(02)00108-6

[4] M.A. Penny, R. Verity, C.A. Bever, C. Sauboin, K. Galactionova, S. Flasche, M.T. White, E.A. Wenger, N. Van de Velde, P. Pemberton-Ross, J.T. Griffin, T.A. Smith, P.A. Eckhoff, F. Muhib, M. Jit and A.C. Ghani, Public health impact and cost-effectiveness of the RTS,S/AS01 malaria vaccine: a systematic comparison of predictions from four mathematical models, *The Lancet*, 387 (10016) (2016), 367–375. https://doi.org/10.1016/S0140-6736(15)00725-4

[5] R. Resmawan and L. Yahya, Sensitivity analysis of mathematical model of Coronavirus Disease (COVID-19) transmission, *CAUCHY*, 6 (2020), 91–99. *https://doi.org/10.18860/ca.v6i2.9165*

[6] R. Resmawan and Nurwan, Konstruksi Bilangan Reproduksi pada Model Epidemik SEIRS-SEI Penyebaran Malaria dengan Vaksinasi dan Pengobatan, *Jurnal Matematika Integratif*, 13 (2) (2017), 105–114.

[7] D.L. Smith, J. Dushoff and F.E. McKenzie, The risk of a mosquito-borne infection in a heterogeneous environment, *PLoS Biology*, 2 (11) (2004), e368. https://doi.org/10.1371/journal.pbio.0020368

[8] C. Castillo-Chavez and B. Song, Dynamical models of tuberculosis and their applications, *Mathematical Biosciences and Engineering*, 1 (2) (2004), 361–404. https://doi.org/10.3934/mbe.2004.1.361

[9] J.C. Butcher, *Numerical Methods for Ordinary Differential Equations*, 3rd ed., John Wiley & Sons, Chichester, 2016. https://doi.org/10.1002/9781119121534